Available online at www.sciencedirect.com
ScienceDirect
Journal of Power Sources 159 (2006) 1042–1047
JOURNAL OF POWER SOURCES
www.elsevier.com/locate/jpowsour

Development of a small DMFC bipolar plate stack for portable applications

C.Y. Chen *, J.Y. Shiu, Y.S. Lee

Institute of Nuclear Energy Research (INER), No.1000, Wunhua Rd., Jiaan Village, Longtan Township, Taoyuan County 32546, Taiwan, ROC

Received 21 October 2005; received in revised form 9 December 2005; accepted 12 December 2005
Available online 9 February 2006

Abstract

The direct methanol fuel cell (DMFC) is regarded as a promising candidate in portable electronic power applications. Bipolar plate stacks were systematically studied by controlling the operating conditions, and by adjusting the stack structure design parameters, to develop more commercial DMFCs. The findings indicate that the peak power of the stack is influenced more strongly by the flow rate of air than by that of the methanol solution. Notably, the stack performance remains constant even as the channel depth is decreased from 1.0 to 0.6 mm, without loss of the performance in each cell. Furthermore, the specific power density of the stack was increased greatly from ~60 to ~100 W l^{-1} for stacks of 10 and 18 cells, respectively. The current status of the work indicates that the power output of an 18-cell short stack reaches 33 W in air at 70 °C. The outer dimensions of this 18-cell short stack are only 80 mm × 80 mm × 51 mm, which are suitable for practical applications in 10–20 W DMFC portable systems.

Keywords: Direct methanol fuel cell; Membrane electrode assembly; Power density; Portable

1. Introduction

Although the high cost of fuel cell systems has hindered their commercialization, fuel cell systems have received much attention in recent years [1–5] because of the increasing price of petroleum and the expectation that fuel cells will serve as the next generation of power sources with the advantages of high efficiency and low pollution. Among various kinds of fuel cells, the direct methanol fuel cell (DMFC) is considered to be an energy source with potential for use in portable electronic devices such as mobile phones, laptop computers and other advanced mobile electronic devices, because it has a high energy density and a low operating temperature, and uses liquid fuel and current supply infrastructure [6–10]. These advantages enable simple and safe handling and a low-cost distribution system. However, the DMFC suffers from a lower power density than that of the proton exchange membrane fuel cell (PEMFC) which uses hydrogen. Therefore, the performance of DMFCs must be enhanced either by developing better membrane electrode assemblies (MEAs) or by improving the stack structure design to increase the specific power density (W l^{-1} or W kg^{-1}). Many single cells can be simply assembled together (in what is known as a stack) to increase the stack performance and to meet the voltage requirements for practical applications. Most researchers have concentrated on polymer electrolyte membrane fuel cell stacks with a wide range of types and functions [11–15]. Fuel cell stacks can be classified into three major types: bipolar plate, pseudo bipolar electrode and monopolar strip stacks, based on the differences among electrode units in the stack design [14]. Much effort has been made on understanding PEMFC bipolar plate stacks. However, relatively little effort has been made to understand the DMFC bipolar plate stacks [16,17], because the pseudo bipolar electrode and monopolar strip stacks for an air-breathing DMFC are very attractive for use in portable applications because air compressors can be simply removed. However, the flooding problem, which significantly affects the long-term stability of operation, is a major limitation of air-breathing DMFCs [6]. Consequently, the main objective of this program is to explore the performance of a DMFC bipolar plate stack and demonstrate that the DMFC stack can also be made in a compact size that is appropriate

* Corresponding author. Tel.: +886 3 4711400x6653; fax: +886 3 4711409.
E-mail address: cychen@iner.gov.tw (C.Y. Chen).

0378-7753/$ – see front matter © 2006 Elsevier B.V. All rights reserved.
doi:10.1016/j.jpowsour.2005.12.017

for practical applications in 10–20 W DMFC portable power systems. In this work, a small DMFC stack, exhibiting high performance because of a thin bipolar plate, is manufactured by increasing the number of cells in a stack, and by adjusting the operating conditions (such as flow rate of methanol/air and temperature). The stack performance was analyzed by measuring the maximum power density from current–voltage characteristics. This study shows that the power densities of a 10- and 18-cell short stack were almost the same, even if the thickness of bipolar plate is considerably reduced from 3.0 to 1.7 mm. The power output of an 18-cell short stack with dimensions of only 80 mm × 80 mm × 51 mm can reach 33 W at 70 °C in air.

2. Experimental

2.1. Fabrication of the membrane electrode assembly

The MEAs, which consist of electrodes and the electrolyte membrane, were prepared by the same procedure as that reported in our previous work [18]. The electrode inks for the electrodes were obtained from a mixture of Nafion solution (DuPont), Pt-Ru/C and Pt/C catalysts (Johnson Matthey). The catalysts with mean particle sizes of ∼2.5 nm were supported on a conductive carbon black with a high surface area. The inks were then coated by a screen-printing technique onto each surface of Nafion 117 membranes (DuPont) to make the electrodes. The MEAs were then hot pressed at 120 °C and 50 kg cm^{-2} for 2 min. The electrode area of the MEA was 25 cm^2. The Pt-Ru and Pt loadings were ∼2 and ∼3.5 mg cm^{-2} in anode and cathode, respectively.

2.2. Stack design and assembly

The DMFC stack was built from the above MEAs, carbon cloths, gaskets and machined graphite bipolar plates. The MEA was sandwiched between carbon cloths (used as diffusion layers) and then installed in a bipolar plate stack with two current collectors positioned at each end of the stack. Teflon gaskets were placed between bipolar plates to prevent liquid and gas leakage to the exterior and cross leakage between the fluids in stack. Serpentine type flow fields were used for fuel distribution on anode and cathode sides. The current collectors were made from a stainless steel or a titanium alloy. During the development process, the stack construction was changed as a result of stack performance testing under various operating conditions. Two bipolar plate thicknesses of 3 and 1.7 mm were tested. Careful evaluation of the stack structure yielded a very compact design without sacrificing the performance of each cell.

2.3. Stack testing

The stack performance was evaluated by measuring the current–voltage (polarization curves) and the current–power characteristics using a test station equipped with a Chroma 63030 electronic load. The test station allowed measurement and recording of voltage, current and temperature. In the test station, a 3 wt.% aqueous methanol solution at elevated temperature and air with various flow rates at room temperature were fed to the anode and cathode, respectively; the temperature of the methanol solution was measured at the outlet of the anode compartment. The fuel cells were assembled into a 10-, 16- and 18-cell arrangement where one input manifold was used to feed methanol solution to all the anode flow fields and another input manifold to feed air to all the cathode flow fields. Fig. 1 shows an experimental 18-cell bipolar plate stack.

Fig. 1. An experimental 18-cell bipolar plate stack.

3. Results and discussion

A systematic study of the effects of operating conditions (such as temperature, flow rate of methanol solution and air) and stack structure design parameters (including gas diffusion layer characteristics, gasket thickness and channel depth) on stack performance is described as follows.

3.1. Effect of flow rate of air and the methanol solution

The flow rate of air at the cathode has a crucial influence on stack performance. Fig. 2 shows the effect of three different flow rates of air on the 16-cell stack performance tested with a 3 wt.% methanol solution at 70 °C and a flow rate of 130 ml min^{-1}. The effect of the air flow rate on the peak power as determined from the polarization curves in Fig. 2 is shown in Fig. 3. The peak power increased as the air flow rate increased from 6 to 12 l min^{-1}. This is because most of water produced at the cathodes was removed, the O_2 mass transport (concentration) increased, and the methanol crossover problem was lessened by a sufficient air supply to the cathode side.

Fig. 4 shows the effect of three different flow rates of the methanol solution on the 16-cell stack performance tested with 3 wt.% methanol solution at 70 °C and 9 l min^{-1} of air at room temperature. The variation of peak power with flow rate of the methanol solution is plotted in Fig. 5. The peak power increased slowly as the flow rate of methanol solution was increased from 80 to 130 ml min^{-1} and then changed little at a high flow rate of 200 ml min^{-1}. Notably, the peak power was influenced more

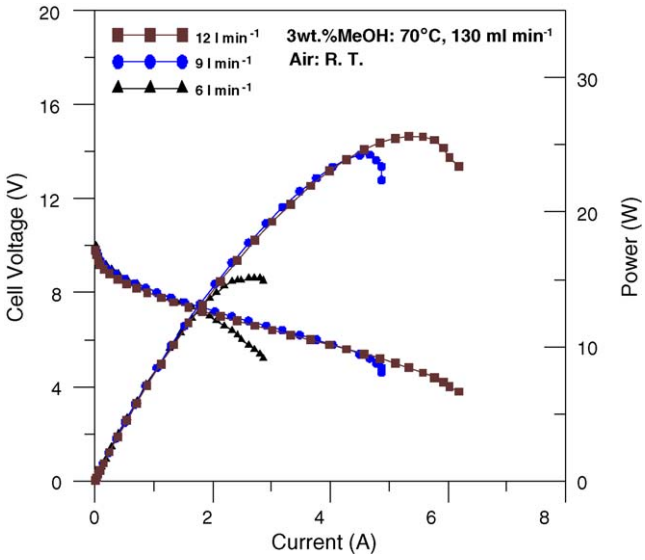

Fig. 2. Effect of flow rate of air on the 16-cell stack performance.

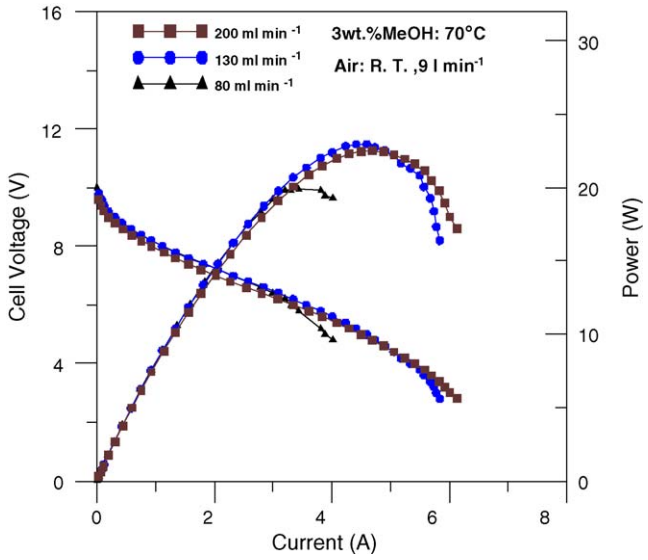

Fig. 4. Effect of the flow rate of methanol solution on the 16-cell stack performance.

significantly by the flow rate of air than by that of the methanol solution, as clearly indicated by the steep rise in peak power in Fig. 3 and the gentle rise in Fig. 5.

3.2. Effect of temperature of methanol solution

For practical purposes, we evaluate the effect of the methanol solution temperature on the 16-cell stack performance tested with sufficient air (at a flow rate of 9 l min^{-1}) at room temperature, as seen from Fig. 6. As expected, the stack performance increased with temperature because the rate of electrochemical reaction increased with temperature. Since the rate of the electrochemical reaction is directly related to the activation polarization, the activation loss will decrease as the electrochemical reaction rate increases. Close inspection of the current–voltage curves in Fig. 6 shows that the activation polarization is dominant at low current and the activation loss is less at 70 °C than at 50 °C.

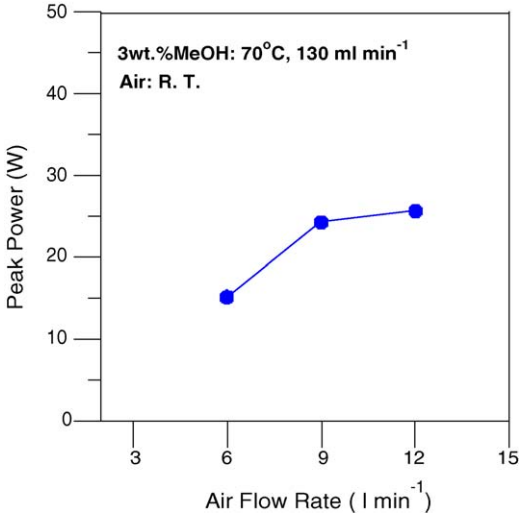

Fig. 3. Variation of peak power with the flow rate of air.

3.3. Effect of the gas diffusion layer

The influence of the wet proofing in the gas diffusion layer on the cathode side was investigated since the cathode mass transport involves both gas and liquid phase. The normal carbon cloths and Teflon-treated carbon cloths, purchased from ElectroChem. Inc., were chosen as diffusion layers. Fig. 7 shows the effect of carbon cloth characteristics at the cathode side on the 10-cell stack performance. The stack performance with the gas diffusion layer containing Teflon might perform a little worse than the untreated one. This result was ascribed to the high electrical resistance when adding Teflon to the gas diffusion layer. By a close examination of the current–voltage curves in Fig. 7, one can easily understand how Teflon-coated carbon cloth affect the ohmic polarization (loss) in the medium current range.

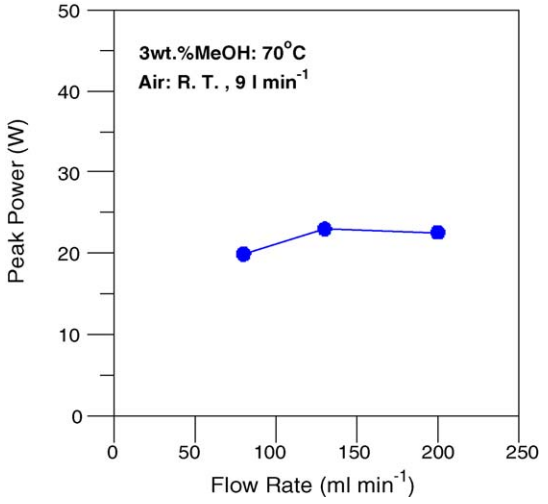

Fig. 5. Variation of peak power with the flow rate of the methanol solution.

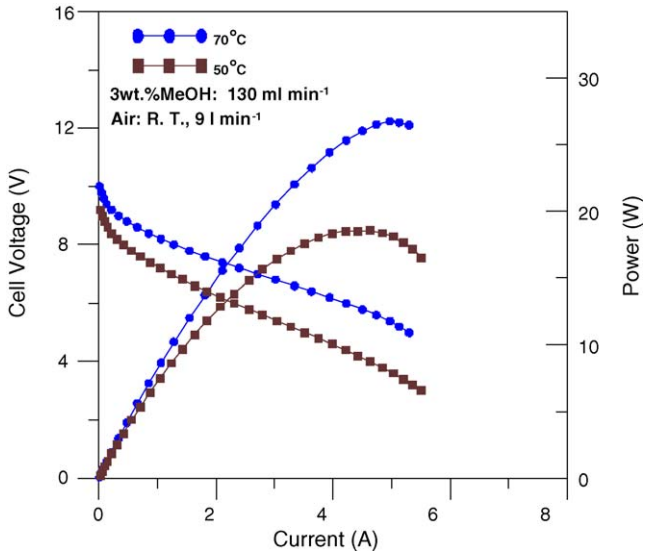

Fig. 6. Effect of temperature of the methanol solution on the 16-cell stack performance.

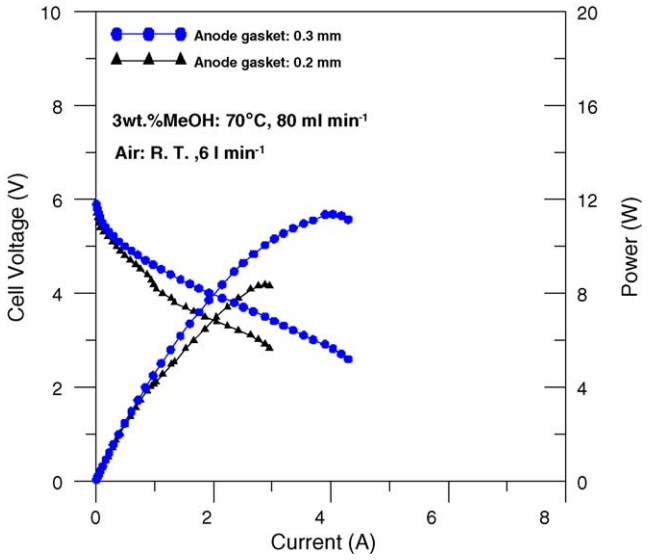

Fig. 8. Effect of gasket thickness at the anode side on the 10-cell stack performance.

3.4. Effect of gasket thickness

We also study the effect of the gasket thickness that may result when a stack is assembled. Namely, the porosity of diffusion layers may change depending on the thickness of gasket when the fixed amount of force is exerted on the stack by a set of eight screw bolts. The Teflon material with the thickness of 0.2 and 0.3 mm were used as the gasket at the anode side, while the gasket thickness at the cathode side was kept constant (= 0.3 mm). This enabled assessment of the effect of gasket thickness at the anode side. A comparison of the polarization curves of the stack performance with these two gaskets of different thickness is illustrated in Fig. 8. The stack performance differences must have originated from the porosity of the diffusion layer. Since the diffusion layer (i.e. carbon cloth) was a porous and compressible material, its porosity decreased and thus the mass transfer resistance increased as the gasket thickness decreased. The mass transfer resistance could be a result of local methanol concentration polarization. As expected, Fig. 8 shows the lower performance of the stack with 0.2 mm anode gasket than that with 0.3 mm one. Interestingly, the experimental result indicated that a concentration polarization could happen even in the low current range. We suppose that the thinner gasket results in either some of the reaction area being blocked or water being excluded from the membrane. This might result in a concentration polarization even at low current densities. A similar phenomenon was observed elsewhere [19].

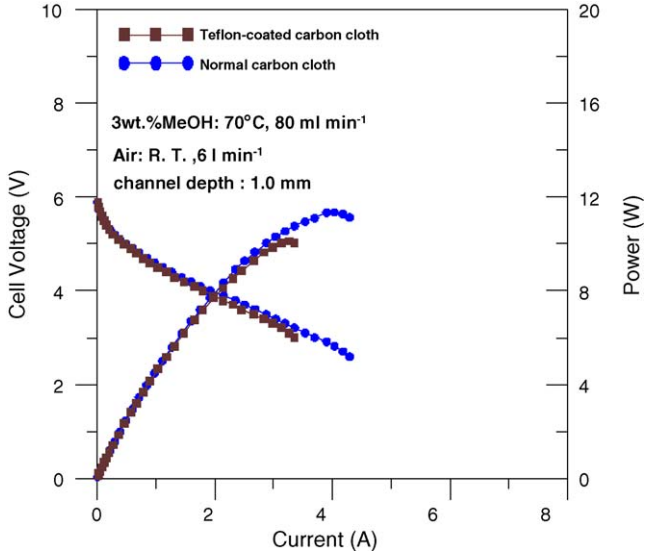

Fig. 7. Effect of carbon cloth characteristics at the cathode side on the 10-cell stack performance.

3.5. Effect of channel depth of bipolar plate

Among many stack design parameters, the channel depth is another important design parameter influencing the stack performance because a change in the channel cross sectional area may lead to a change in the mass transport, the fluid velocity and the fraction of the two phases (gas and liquid phase), thus affecting stack performance. We evaluated the effect of three different channel depths (1.0, 0.6 and 0.5 mm) on the 10-cell stack performance, while keeping the same open ratio of the bipolar stack. The polarization curves corresponding to these channel depths are plotted in Fig. 9. The results show that for a given operating condition, a decrease in the flow channel depth from 1.0 to 0.6 mm leads to the same stack performance. This finding is contrary to the study in the article [20] that a reduction in the anode flow channel depth from 3.0 to 0.5 mm led to a significant improvement in cell performance. This difference in behavior is not surprising because the cell and stack performance depend on the structures of membranes, electrodes, MEA, stack design and even on the operating conditions, which are quite different in the two studies. For the DMFC structure used in this study, the cell performance is not simply enhanced by the decreases in channel depth for the range between 1.0 and 0.6 mm. Fig. 9 also

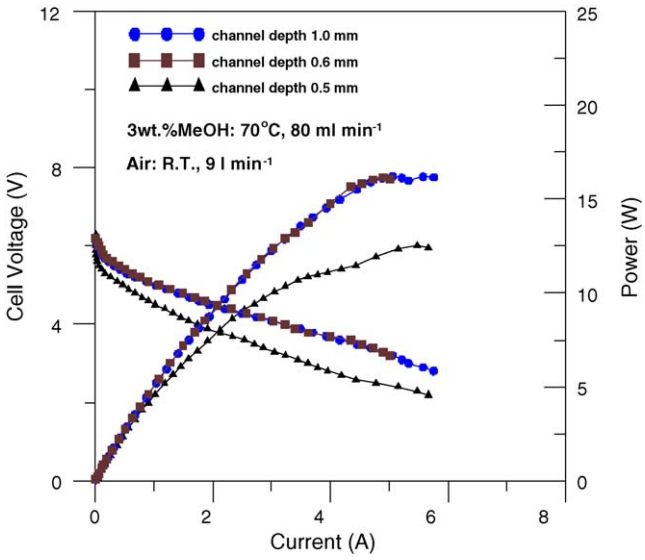

Fig. 9. Effect of channel depth of the bipolar plate on the 10-cell stack performance.

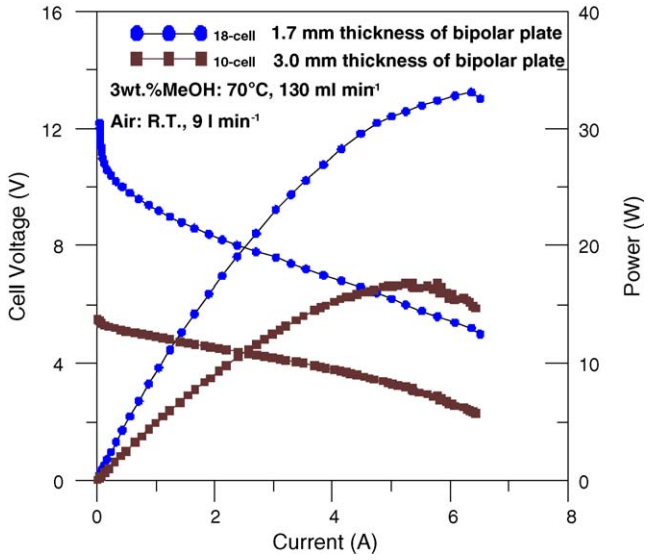

Fig. 11. Stack performance of the 10- and 18-cell stacks with bipolar plate thicknesses of 3.0 and 1.7 mm, respectively.

shows that a further decrease in channel depth to 0.5 mm which resulted in a deterioration in the stack performance. This may be attributed to a mass transport problem, although the decrease in the channel depth should enhance the cell performance because a shallow channel means a high methanol flow rate, which is beneficial to the CO_2 removal and methanol diffusion to the catalyst surface, there must be a limit value for the decreases in channel depth. In our study, 1.0–0.6 mm may be an optimum range. We have demonstrated that the stack performance was retained even as the channel depth is reduced from 1.0 to 0.6 mm. This enables the finding of the optimum channel depth of the stack for a given operating condition and a fixed stack structure design.

3.6. Fabrication of a bipolar plate stack for portable applications

To increase the maximum power output of the stack, one can simply increase the cells in the stack. Fig. 10 shows the 10- and 16-cell stack performance. Apparently, the stack power output is increased with increasing the cells without sacrificing cell performance. Based on the experimental results described above, the optimization of the stack performance can be explored by adjusting the operating conditions, gasket thickness, channel depth (bipolar plate thickness) and the cells in the stack assembled. Fig. 11 shows the stack performance of the 10- and 18-cell stacks with bipolar plate thicknesses of 3.0 and 1.7 mm, respectively. It was demonstrated that stack power output was increased significantly from 17 to 33 W at 70 °C in air as the thickness of

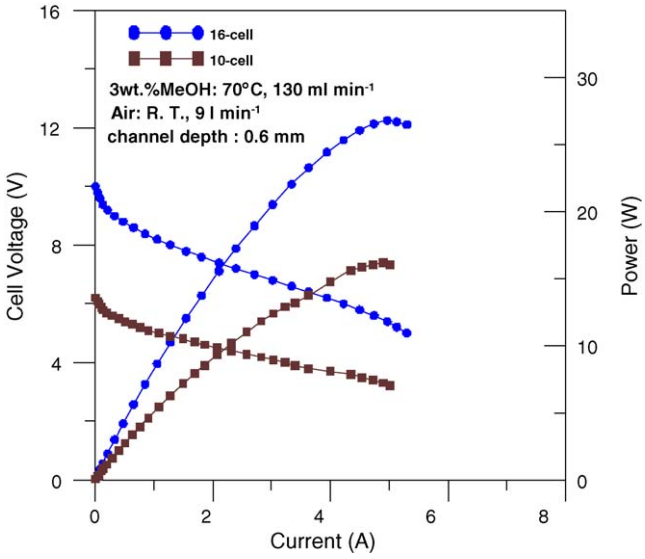

Fig. 10. Stack performance of the 10- and 16-cell stacks.

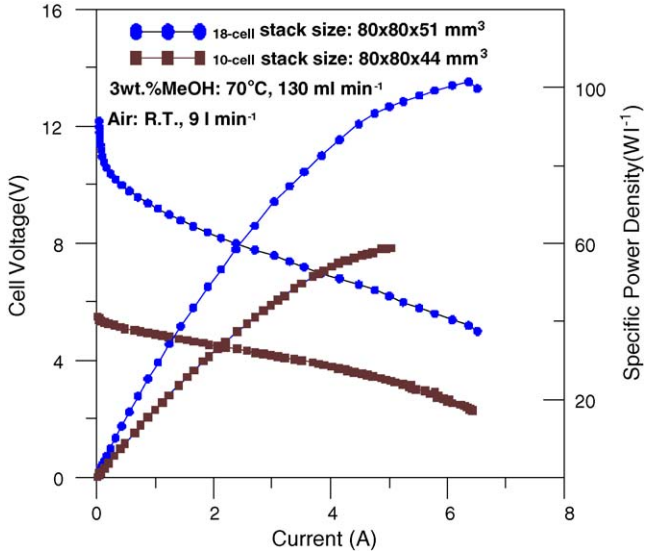

Fig. 12. Specific power densities of the 10- and 18-cell stacks with bipolar plate thicknesses of 3.0 and 1.7 mm, respectively.

the bipolar plate was decreased from 3.0 to 1.7 mm and the cell number was increased from 10 to 18. Since a reduction in the bipolar plate thickness can lead to a reduction in the stack size, the specific power density of the stack can also be increased significantly. Fig. 12 shows that the specific power density of the stack is increased substantially from ∼60 to ∼100 W l^{-1} for a 10-cell stack of 80 mm × 80 mm × 44 mm and an 18-cell stack of 80 mm × 80 mm × 51 mm, respectively.

4. Conclusions

The stack performance was studied systematically by modifying such parameters as temperature, flow rate of the air/methanol solution, the characteristics of the diffusion layer, the gasket thickness and the depth of the channel. The following results are obtained:

1. The peak power of the stack is influenced more significantly by the flow rate of air than the methanol solution.
2. The stack performance with the currently used Teflon-treated carbon cloth might perform a little worse than an untreated one because of the high electrical resistance when the Teflon is added to the gas diffusion layer on the cathode side.
3. The diffusion layer is a porous and compressible material, so the stack performance is influenced by the thickness of the Teflon gasket because this thickness affects the porosity and the mass transfer resistance of the diffusion layer.
4. The stack performance is retained even as the channel depth is reduced from 1.0 to 0.6 mm without degrading the performance in each cell. Since a reduction in the channel depth can lead to a reduction in the bipolar plate thickness, the specific power density of the stack can be increased greatly from ∼60 to ∼100 W l^{-1} for the stack size of 10- and 18-cell, respectively.

This work has demonstrated that a high performance bipolar plate stack can be obtained in a compact size which is suited to portable DMFCs by minimizing the thickness of the bipolar plate and increasing the number of cells in the stack. The power output of a 18-cell short stack with bipolar plate thickness of 1.7 mm can reach 33 W with air operation at 70 °C. The outer dimensions of the 18-cell short stack are only 80 mm × 80 mm × 51 mm. The experimental results indicate that an 18-cell short stack is sufficiently good for practical applications in 10–20 W DMFC portable systems.

Acknowledgement

The authors would like to thank the Institute of Nuclear Energy Research (INER) for financially supporting this research.

References

[1] C. Song, Catal. Today 77 (2002) 17.
[2] J.M. Ogden, M.M. Steinbugler, T.G. Kreutz, J. Power Sources 79 (1999) 143.
[3] A. Lokurlu, T. Grube, B. Höhlein, D. Stolten, Int. J. Hydrogen Energy 28 (2003) 703.
[4] M.A.J. Cropper, S. Geiger, D.M. Jollie, J. Power Sources 131 (2004) 57.
[5] R. Dillon, S. Srinivasan, A.S. Arico, V. Antonucci, J. Power Sources 127 (2004) 112.
[6] C.Y. Chen, P. Yang, J. Power Sources 123 (2003) 37.
[7] A. Blum, T. Duvdevani, M. Philosoph, N. Rudoy, E. Peled, J. Power Sources 117 (2003) 22.
[8] B.-D. Lee, D.-H. Jung a, Y.-H. Ko, J. Power Sources 131 (2004) 207.
[9] J. Han, E.-S. Park, J. Power Sources 112 (2002) 477.
[10] D. Kim, E.A. Cho, S.-A. Hong, I.-H. Oh, H.Y. Ha, J. Power Sources 130 (2004) 172.
[11] T.V. Nguyen, M.W. Knobbe, J. Power Sources 114 (2003) 70.
[12] J. Scholta, N. Berg, P. Wilde, L. Jörissen, J. Garche, J. Power Sources 127 (2004) 206.
[13] J.S. Cooper, J. Power Sources 129 (2002) 152.
[14] R. Jiang, D. Chu, J. Power Sources 93 (2001) 25.
[15] D. Chu, R. Jiang, J. Power Sources 80 (1999) 226.
[16] C. Xie, J. Bostaph, J. Pavio, J. Power Sources 136 (2004) 55.
[17] H. Dohle, H. Schmitz, T. Bewer, J. Mergel, D. Stolten, J. Power Sources 106 (2002) 313.
[18] C.Y. Chen, P. Yang, Y.S. Lee, K.F. Lin, J. Power Sources 141 (2005) 24.
[19] W.K. Lee, C.H. Ho, J.W. Van Zee, M. Murthy, J. Power Sources 84 (1999) 45.
[20] H. Yang, T.S. Zhao, Q. Ye, Electrochem. Commun. 6 (2004) 1098.